Final Draft
of the original manuscript:

Zander, T.; Wieland, D.C.F.; Raj, A.; Salmen, P.; Dogan, S.; Dedinaite, A.; Haramus, V.M.; Schreyer, A.; Claesson, P.M.; Willumeit-Roemer, R.:
Influence of high hydrostatic pressure on solid supported DPPC bilayers with hyaluronan in the presence of Ca2+ ions.
In: Soft Matter. Vol. 15 (2019) 36, 7295 - 7304.
First published online by Royal Society of Chemistry: 04.09.2019

https://dx.doi.org/10.1039/C9SM01066A

Influence of high hydrostatic pressure on solid supported DPPC bilayer with HA in the presence of Ca^{2+} ions

Thomas Zander [a], D.C. Florian Wieland [a,], Akanksha Raj [b], Paul Salmen [d], Susanne Dogan [d], Andra Dėdinaitė [b,c], Vasil M. Garamus [a], Andreas Schreyer [a], Per Martin Claesson [b,c], Regine Willumeit-Römer [a]*

[a] Helmholtz-Zentrum Geesthacht: Centre for Materials and Costal Research, Institute of Materials Research, Max-Planck-Straße 1, 21502 Geesthacht, Germany

[b] KTH Royal Institute of Technology, School of Chemical Sciences and Engineering, Department of Chemistry, Surface and Corrosion Science, Drottning Kristinas väg 51, SE-10044 Stockholm, Sweden

[c] SP Technical Research Institute of Sweden, SP Chemistry, Materials and Surfaces, Box 5607, SE-114 86 Stockholm, Sweden

[d] Fakultät Physik/DELTA, TU Dortmund, 44221 Dortmund, Germany

KEYWORDS

High Pressure, X-Ray Reflectivity, Hyaluronan, Solid Supported DPPC, Synovial Joint, Fluorescent Microscopy

ABSTRACT

The molecular mechanisms responsible for outstanding lubrication of natural systems, like articular joints, have been in the focus of scientific research for several decades. Despite all the efforts made, the lubrication mechanisms are not yet completely understood. One important aspect is the lubrication of such systems under high pressure, where it is important to identify how lubricating entities adapt under dynamic working conditions to maintain their performance. Thus, to simulate the situation at the cartilage surface under high load, we investigated a model system of the cartilage interface consisting of layers of 1, 2-dipalmitoyl-sn-glycero-3-phosphocholine (DPPC) and hyaluronan (HA) at high hydrostatic pressure. Phospholipid layers are found at the cartilage surfaces and are able to considerably reduce friction and wear. Their behavior under high hydrostatic pressure and varied solutions conditions is important as pressures of 200 bar are encountered during daily life activities. In the present investigation we particularly focus on how divalent ions, like Ca^{2+}, affect the interaction between DPPC and HA, as other investigations have indicated that calcium ions affect the interaction between these two components. To obtain structural information we studied the sample system in solutions containing NaCl and $CaCl_2$, using X-ray reflectivity and fluorescence microscopy. It could be shown that HA strongly influences the DPPC bilayer structure in the presence of Ca^{2+}.Our results suggest that the calcium ions increase the robustness of the DPPC layer against pressure.

Further, we observe a modification of the DPPC phase diagram as HA absorbs to the bilayer which results in an L_α like structure at low temperatures and a decoupling of the upper and lower leaflet under high pressure.

Introduction

Synovial joints exhibit exceptionally good lubrication properties with friction coefficients as low as 0.002-0.006 even under high shear rates and high loads.[2, 3] Lubrication of the cartilage surfaces, which are covered with multilamellar lipid layers[4], is facilitated by the synovial fluid and in particular molecules located at the cartilage surface. The lubrication seems to be realized by a synergistic action of several mechanisms and components.[5] An important premise for good lubrication performance is suggested to be the presence of a tenaciously fluid water layer between the sliding surfaces that is maintained by the biolubricants.[6]

The synovial liquid is a multicomponent system that contains phospholipids, biopolymers (Hyaluronan), proteins (mainly albumin), proteoglycans such as lubricin (also known as PRG4), and ions.[4, 6] Hyaluronan (HA) and phospholipids are thought to be of high importance for the lubrication[7-9], and several studies have shown that phospholipid layers, as found on the surface of the cartilage, are very efficient in reducing boundary friction.[10, 11] Further, HA on its own also reduces friction to a certain extent,[12] and it plays an important role for the rheological properties of the synovial fluid as it controls the viscosity. HA has also been suggested to reduce wear.[13, 14] Injections of HA are used to alleviate osteoarthritis, although the effectiveness is under debate,[15] and it has been reported that mixtures of HA and phospholipids are more efficient than phospholipids alone.[16] Studies at atmospheric pressure have reported an interaction of HA with solid supported 1,2-dipalmitoyl-sn-glycero-3-phosphocholine (DPPC), the most abundant

saturated phospholipid in the synovial joint area. It has been emphasized that the presence of HA allows accumulation of a large amount of phospholipids on the surface,[17, 18] and friction coefficients as low as 0.006 was reported for composite layers adsorbed from solutions containing both DPPC and HA. [19]

HA is a linear polysaccharide, consisting of a repeating disaccharide unit of β1-4 D-glucuronic acid and β1-3 N-acetyl-D-glucosamine,[20] with a persistence length close to 9 nm in 150mM NaCl.[21] The polymer chains form network structures in aqueous solutions due to entanglements and the presence of hydrophobic patches.[22] In aqueous solutions at physiological pH-values HA is highly negatively charged due to dissociation of its carboxylic acid groups, the pKa of which is reported to be in the range 3-4,[23] and globally it forms a coiled structure.[22] DPPC is an amphiphilic molecule with a zwitterionic, hydrophilic headgroup of phosphatidylcholine and two hydrophobic palmitic acid chains (the 'tailgroup'). DPPC molecules self-assemble into layered structures when in contact with excess water. Depending on pressure and temperature these DPPC-structures can be found in different phases. The most important ones are the the gel ($L_{\beta'}$), ripple ($P_{\beta'}$) and fluid (L_{α}) phase.[24] In the $L_{\beta'}$ phase the alkyl chains of the lipids are in an all-trans configuration with a chain tilt angle of about 32 °,[25] whereas in the L_{α} phase the chains are molten and have some local cis-conformations.[26] Thus, the bilayer thickness is reduced in the L_{α} phase compared to that of the $L_{\beta'}$ phase. The $P_{\beta'}$ phase is more complicated and its structure has only recently been better understood.[27] In this phase the layer is partly molten, where melting occurs along straight lines at the bilayer surface. The bilayer forms periodic ripples due to the differences in thickness between the molten lines and the rest of the bilayer. Some previous studies have demonstrated that solid supported bilayers do not show a $P_{\beta'}$ phase,[28, 29] but other studies suggest the existence of a ripple phase also for such bilayers.[30, 31] At ambient pressure,

for DPPC, the transition from the $L_{\beta'}$ to the $P_{\beta'}$ phase occurs at around 34 °C in bulk solution, and the transition from the $P_{\beta'}$ to the L_{α} phase occurs at around 41 °C.[26] Changes in pressure induce a shift in the phase transitions to higher values by 22 °C / kbar.[32]

The studies of the lubrication properties of silica supported DPPC/HA mixtures revealed only very limited information on the molecular arrangement of the two components through AFM imaging.[17, 18] Further, the influence of hydrostatic pressure, which plays an important role in joint lubrication in the case of high loads that pressurize the synovial joints, was not investigated. During normal activity pressures up to 180 bar (18 MPa) have been measured in human hip joints.[33] The self-assembly of DPPC and HA and the effect of high hydrostatic pressures have already been determined by X-ray reflectivity (XRR) measurements of silica supported DPPC/HA composites at different hydrostatic pressures (up to 2000 bar).[34] The results indicated that HA stabilizes silica supported DPPC bilayers at high hydrostatic pressures. The samples were studied in a solution that contained only 150 mM NaCl. However, the synovial fluid contains also other ions, e.g., calcium ions at a concentration of about 5 mM.[35] It is known that divalent ions like calcium affect the packing of DPPC[8, 36] along with their hydration.[37] Further, calcium ions have a strong influence on the interaction of DPPC and HA,[38] where we observed a large difference in the supramolecular structure after adding $CaCl_2$ (c_{CaCl2} = 10 mM) into the solution.

In this work, we pursue the question if and how calcium ions influence the structure of DPPC/HA composite layers at high hydrostatic pressures. To this end, we performed XRR measurements at two different temperatures (39 °C and 55 °C) and pressures up to 2000 bar. Further, HA of two different molecular weights was used as it is assumed that the molecular

weight plays a role in arthritis.[39] Additionally, fluorescence microscopy images were recorded to obtain information on the lateral organization on the micrometer scale.

Experimental section

Material

DPPC was purchased from Avanti polar lipids (catalogue No. 850355P), and HA was bought from Creative PEGworks. HA samples with a weight averaged molecular weights of 10 kDa (catalogue No. HA-101) and 1500 kDa (catalogue No. HA-106) were used. All compounds were used as received. In the following HA with a MW of 1500 kDa will be referred to as HA1500 and HA with a MW of 10 kDa as HA10. Sodium chloride (assay ≥99.8, catalogue No. 31434, purchased from Sigma-Aldrich), calcium chloride dehydrate (assay ≥99, catalogue No. 5239, purchased from Carl Roth) and ultrapure water (Milli-Q, 18.2 MΩ cm) were used to prepare solutions with NaCl and $CaCl_2$.

Labelled DPPC (NBD-DPPC) was purchased from Avanti polar lipids (catalogue No. 810131C) and used in the fluorescent microscopy studies. The marker molecule, 12-[(7-nitro-2-1,3-benzoxadiazol-4-yl)amino]dodecanoyl (NBD), was attached at the end of one of the alkyl chains of DPPC. Fluorescent labelled HA with two different molecular weights (10 kDa and 1500 kDa) was purchased from Creative PEGworks (catalogue No. HA-704 and HA-705). The marker molecule was 5/6-carboxy-tetramethyl-rhodamine.

Silicon wafers with a surface area of 7.5 x 7.5 mm^2 were used as flat substrates. Before usage the Si wafers were cleaned following the RCA-1 cleaning protocol.[40, 41]

Sample Preparation

Solid supported samples composed of DPPC and DPPC/HA were prepared in a stepwise approach as described in detail in our previous article and shortly described herein.[34] Solid supported DPPC bilayers were prepared via vesicle fusion [42, 43] from a solution containing DPPC vesicles with a concentration of 0.5 mg/mL. Vesicles were prepared via extrusion through a membrane with a pore size of 0.2 μm (Whatman catalogue No. 7060-2502). The cleaned silicon wafers were immersed in the vesicles solution and were kept there for 30 min at 55°C. The sample was rinsed with a 150mM NaCl and 10mM $CaCl_2$ salt solution. Then HA was adsorbed to the solid supported DPPC bilayer from a solution containing 0.5 mg/mL HA. The preparation was done at 55 °C. All solutions were prepared with 150 mM NaCl and 10 mM $CaCl_2$. After preparation the samples were transferred to the sample cell. During all preparation steps it was taken care that the sample remained in the solution at all times, thus preventing uncontrolled deposition or desorption of DPPC or HA. The preparation protocol for the fluorescence microscopy measurements was identical to the one described above, except that DPPC was mixed with NBD-DPPC (1%) and fluorescent labelled HA was used.

X-ray reflectivity measurements

X-ray reflectivity, XRR, measurements were performed at the ID 15, ESRF, France [44] using an X-ray energy of 70 keV. A reflectivity sample cell suitable for applying hydrostatic pressure up to 5 kbar was used for the experiments.[45] The temperature was controlled via a refrigerated-heating circulating bath that was connected to the sample cell, allowing accurate control of the sample temperature (± 0.2 K).

The samples were studied at two different temperatures, 39 °C and 55 °C, as previous experiments showed that this is sufficient to probe the sample in all relevant phases.[34] At 55 °C in bulk the pressure-induced main phase transition (from fluid to ripple phase) occurs at 500 bar.[32] For this reason we applied only pressures up to 2 kbar to the sample. Physiologically most relevant are the measurements carried out with the phospholipids in the fluid state. This is because the phospholipid composition found in the synovial joint area includes significant amount of unsaturated species [13, 46] that promote formation of fluid layers. At ambient pressure DPPC can be found in the fluid phase above 41 °C.

X-ray reflectivity data treatment

The specular reflected intensity *I* of the X-ray beam was recorded as function of the incident angle θ. This quantity is determined by the average electron density (ρ_e) of the sample perpendicular to the surface:[47]

$$I(q_z) = R_F \left| \frac{1}{\rho_e(z \to \infty)} \int_{-\infty}^{\infty} \frac{d\rho_e}{dz} e^{iqz} \right|^2,$$

where q denotes the modulus of the wave vector transfer perpendicular to the surface and is given by:

$$q_z = \frac{4\pi}{\lambda} \sin(\theta)$$

R_F denotes the Fresnel reflectivity, which is in this case is the reflectivity of a perfectly flat Si surface in water, λ is the wavelength of the X-rays, and z gives the position perpendicular to the surface of the sample. The specular reflected intensity provides information about the vertical

structure of the sample. The background was determined by subtracting the diffusely scattered intensity yielding the specular reflected scattering signal alone.

To evaluate the data, theoretical scattering curves were calculated and fitted to the experimental data using the Parratt algorithm.[48] Interfacial roughness was accounted for by applying the effective-density model.[49] The software package LSFit was used.

The model of the electron density profiles used for fitting consisted of 6 slabs as shown in Figure 2b. The slabs represent the different sections of the sample in the following order starting with the silicon on the very far left (see Figure 1): silicon, silicon dioxide, phospholipid headgroup and tailgroup of the lower leaflet, CH_3 terminal group, phospholidid tailgroup and headgroup of the upper leaflet. The thickness of the silicon dioxide layer was determined by XRR measurements of the bare Si wafer. Thereby the number of fitting parameters and ambiguities in the fitting process could be minimized. The electron densities of Si and water (at different pressures[50]) were calculated (Table S1). All other parameters were determined from the fitting. To calculate errors for the single parameters they were changed until the value of chi-square was doubled.

Fluorescence Microscopy

A Nikon (Nikon Corporation, Tokyo, Japan) Eclipse Ni-E instrument was used to take microscopy images (resolution: 0.23 μm/pixel). Two filter blocks from Semrock Inc (Rochester, USA) were used to visualize the fluorescent markers: i) for NBD-DPPC a filter block which emits blue and detects green light (FITC-3540C) was used, and ii) for rhodamine labelled HA a filter block emitting green and detecting red light (TXRED-4040C) was employed. The measurements were performed at room temperature.

Results and Discussion

Lateral structure of DPPC/HA layers

Images showing the lateral organization of silica supported DPPC and DPPC/HA samples in 150 mM NaCl with 10 mM $CaCl_2$, recorded via fluorescence microscopy, are shown in Figure 1. The used markers show DPPC in green and HA in red. As the wafer with DPPC and HA10 was slightly tilted during the measurements the complete field of view was not in the focal plane, which is just possible to notice in Figure 1. Images A-C in Figure 1 show that the wafers are completely covered with DPPC in all cases. In the presence of HA (images B and C) the coverage appears less homogenous than for pure DPPC (images A). It also seems that HA1500 (image C) has a stronger impact on the lateral distribution of DPPC than HA10 (image B). Measurements of DPPC alone showed a slight red and homogeneous background (image D) that differed significantly from the structures seen for DPPC/HA samples (images E and F). Thus, it can be concluded that the signal seen for DPPC/HA sample stems from the labelled HA that adsorbed to the DPPC bilayer. The coverage of HA appears to be inhomogeneous with some strikingly bright red spots suggestive of accumulations of HA. To visualize a co-localisation of DPPC and HA, the images where thresholded and the resulting images where superimposed (G-I). For a better visualisation the colours of DPPC was changed from green to blue. These images indicate co-localisation as most of the blue spots (DPPC) are next to red spots (HA). Comparing the images to results from Zander et al.,[34] obtained in 150 M NaCl in absence of calcium ions, it can be observed that the fluorescence microscopy images show a similar lateral structure of DPPC and DPPC/HA in contact with a solution containing 150 mM NaCl and one containing 150 mM NaCl and 10 mM $CaCl_2$.[34] However, the intensity of the HA signal observed in the

images reported here is much stronger indicating a higher adsorption in presence of calcium ions. This hints at a stronger interaction of HA and DPPC in the presence of Ca^{2+} ions, as also shown at the water-air interface by Wieland et al.[38]

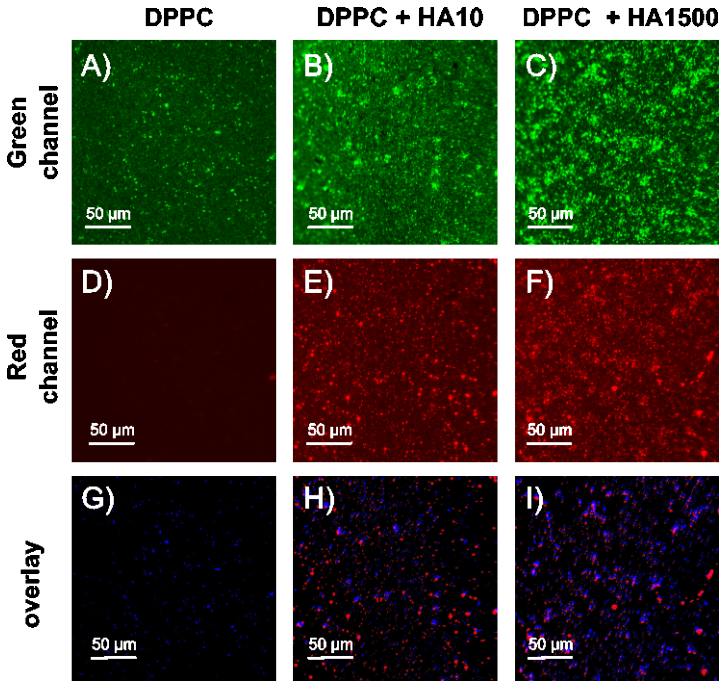

Figure 1 Fluorescence microscopy images of silica supported DPPC bilayers and DPPC/HA composites in contact with aqueous solutions containing 150 mM NaCl and 10 mM $CaCl_2$. DPPC is labeled with a green and HA with a red marker. The scale bars are 50 µm. Images G-I show a super position of the single channels to check for co-localization. For a better visibility the color of DPPC was changed from green to blue.

Phase behaviour of supported DPPC bilayers

In order to understand how HA interacts with a solid supported DPPC bilayer and alter its structure it is necessary to first consider the DPPC bilayer in NaCl/$CaCl_2$ solution without the

influence of HA. Therefore, solid supported DPPC bilayers were studied at 39 °C and 55 °C and at different hydrostatic pressures between 60 and 2000 bar. The samples were probed at 60, 100, 500, 1000 and 2000 bar, and afterwards the pressure was lowered and a final measurement was performed at 60 bar (in the following denoted 60 bar D). Fresnel normalized reflectivity curves of the complete pressure cycle together with the fits and the model electron densities are shown in the supporting information (Figures S2 and S3).

Fresnel normalized reflectivity curves with fits and model electron densities for the measurements at four pressure steps at 39 °C and 55 °C are shown in Figure 2a and Figure 2b, respectively. The electron densities are typical of a solid supported bilayer, where the structure of the lower and upper leaflets are close to identical and exhibit pronounced structural features. The profiles show only small changes due to the increased hydrostatic pressures, like a general increased level of the electron density at higher hydrostatic pressure.

In order to have a quantitative value of the bilayer thickness we calculated the head-to-head distances, which is shown in Figure 2c for the complete pressure cycle. At 39 °C only a small variation centred around 4.4 - 4.5 nm can be observed. This values indicates that the DPPC bilayer is in the $L_{\beta'}$ phase at 39 °C,[26, 36, 51] and it does not enter the $P_{\beta'}$ phase as would occurs at 500 bar in bulk solutions. Thus, it seems that the $P_{\beta'}$ phase is suppressed for DPPC bilayers on the solid support,[52, 53] as already argued for silica supported DPPC bilayer in contact with 150 mM NaCl solution without added $CaCl_2$.[34] The shape of the electron density curves supports this finding as rippled phase would induce a strong smearing of the electron density profile. In the $L_{\beta'}$ phase the chains are more ordered and therefore show a more distinct bilayer structure than observed in fluid bilayers.[54]

Electron density profiles of DPPC samples at 55 °C are shown in Figure 2b, and again the

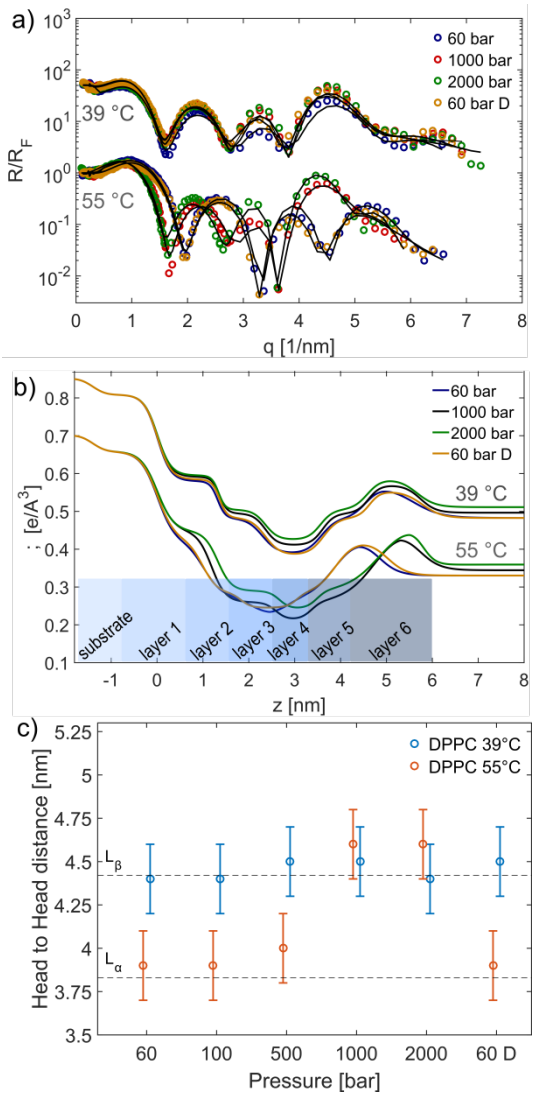

Figure 2 (a) Fresnel normalized reflectivity curves and fits of DPPC samples at 39 °C and 55 °C at different pressures. Offset between 39 °C and 55 °C for clarity. (b) Calculated electron density profiles. Offset between 39 °C and 55 °C for clarity. The layers used for the fitting algorithm are sketched. (c) Head-to-head distances of DPPC for all pressure steps at 39 °C and 55 °C. The aqueous solution contained 150 mM NaCl and 10 mM $CaCl_2$.

typical structure of the lower and upper leaflets are observed. A clear transition can be observed between the profiles recorded at 60 bar and pressures ≥ 1000 bar. At 60 bar the head-to-head distance was found to be 3.9 nm, typical of the value found in the L_α phase. However, it increased to 4.6 nm at 1000 bar, comparable to the values found for DPPC at 39 °C (see Figure 2b). From 1000 bar to 2000 bar the head-to-head distance did not change further. However, small variations in the electron density profile can be seen like a further shift in the position of the gap that separates the single leaflets to larger *z*-values. Besides having different thicknesses, the two states (P≤500 bar and P ≥ 1000 bar) differ in the shape of the electron density profile. At 60 bar the bilayer is more smeared while for ≥ 1000 bar the structural feature of the lower leaflet gets more pronounced which is mostly visible as a decreased roughness of the interface between head group and tail group at z = 1.2 nm. The structural transition, occurring between 500 bar and 1000 bar, is, within error, reversible. Figure 3c summarizes the head-to-head distance as a function of temperature and pressure. The different phases can be easily identified and again no ripple phase is observed, which should be visible in the pressure range between 600 bar and 1500 bar in bulk solution.

XRR data for silica supported DPPC bilayer in 150 mM NaCl solution[34] showed a breakdown of the layer at 55 °C, after the pressure was released from 2000 to 60 bar. In contrast, in the presence of Ca^{2+} ions the electron densities of the bilayer show a reversible transition and the original shape of the bilayer was restored after the pressure was released. It seems likely that the presence of Ca^{2+} ions lead to a stabilization of the bilayer by binding to the negatively charged phosphate groups of the different DPPC molecules.[36, 55-57] Further, it is known that Ca^{2+} ions do alter the properties of solid supported bilayers as they interact with the lipids and the surface.[58]

Structure of supported DPPC bilayers in presence of HA

The electron density profiles of DPPC with adsorbed HA at 60 bar at 39 °C, obtained from the fits of the reflectivity curves, are plotted in Figure 3a. The samples composed of DPPC with HA show a less pronounced structure than samples of DPPC alone, especially the sample with HA10, which can be understood by adsorption of HA to the DPPC bilayer. Most interestingly,

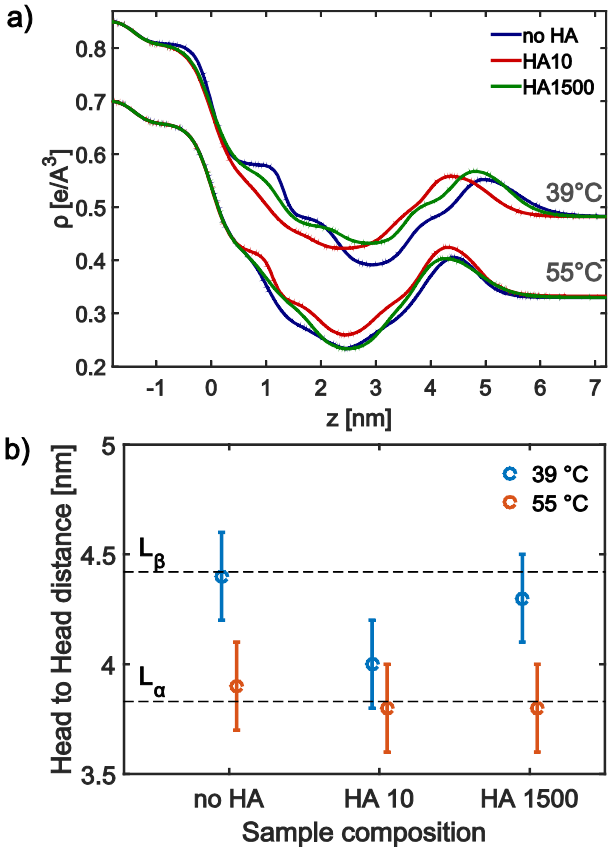

Figure 3 (a) Electron density profiles of DPPC and DPPC with HA (M_W = 10 kDa and M_W = 1500 kDa), recorded at 60 bar and 39 °C and 55 °C. The offset between data obtained at 39 °C and 55 °C is for clarity. (b) Head-to-head distances of DPPC and DPPC/HA samples at 60 bar. The dashed lines show the head-to-head distance of the $L_{\beta'}$ phase (≈ 4.4 nm) and the L_α phase (≈ 3.8 nm).[1] The aqueous solution contained 150 mM NaCl and 10 mM $CaCl_2$.

composite samples of DPPC and HA10 have a significantly lower head-to-head distance than the pure DPPC layer (Figure 3b), which is comparable to the thickness of the lone DPPC bilayer in L_α phase at 55 °C. This hints at changed phase behaviour in presence of HA10, which will be discussed in the next section. The DPPC/HA10 and DPPC/HA1500 composite layers also show an asymmetry between the upper and lower leaflet. This can also be seen in the supplementary information, Figure S2 and S3. The electron density of the tail group region of the upper leaflet is strongly increased and considerably higher than the electron density of the lower leaflet. In general, the roughness of the single slabs is higher in the lower leaflet. In contrast, the electron density profile of the lone DPPC sample is essentially similar in the two leaflets. The data obtained at 55 °C, see Figure 3a, display similar, but less pronounced differences to that of the pure DPPC bilayer.

The asymmetry of the two leaflets in presence of HA, and the change in the roughness, is suggested to be due to HA chains penetrating the upper leaflet (HA has a higher electron density than the DPPC tail group). This could further induce a changed packing of the DPPC molecules. This effect is much stronger than observed for DPPC and HA in 150 mM NaCl in absence of $CaCl_2$.[34] Therefore, it must be concluded that Ca^{2+} ions are responsible for the increased interaction. It seems likely that this effect is due to a stronger interaction between the carboxyl group of HA and the phosphate group of DPPC mediated by calcium ion. Different studies have already shown that Ca^{2+} ions adsorb to the negatively charged phosphate group of DPPC.[36, 55-57] Thus, these ions can give rise to a positive net charge of phospholipid aggregates and bilayers, which can strongly attract the negatively charged carboxyl groups of HA. Such an increased accumulation of HA in presence of calcium ions was also observed by Wieland et al., in their study of DPPC monolayers at the air-water interface.[38]

HA10 of low molecular weight induces a slightly higher asymmetry compared to HA1500 with a high molecular weight. This seems to be in contrast to the findings from the fluorescence microscopy images, but it must be kept in mind that the two methods are sensitive to very different effects. While the fluorescence microscopy images show the lateral structure with μm resolution, the XRR gives information along the vertical direction of the bilayer with sub-nm resolution. The reason for the stronger effect of HA10 might be found in its rod like structure.[59] In contrast, HA 1500 shows an overall coiled structure in solution.[60, 61]

Structure of DPPC bilayer with adsorbed HA at high hydrostatic pressures at 39°C

Measurements of samples composed of DPPC with adsorbed HA were performed at high hydrostatic pressures up to 2000 bar at two different temperatures (39 °C and 55 °C). The Fresnel normalized reflectivity curves, fits and electron density profiles can be found in the supporting information, Figures S2 and S3.

The obtained electron density profiles for samples composed of DPPC and HA at 39 °C at four different pressure steps are shown in Figure 4. Clear differences in the electron density profiles can be observed within the pressure cycle, and the structural changes are not completely reversible. We will first discuss the samples with low molecular weight hyaluronan, HA10, and then consider samples with high molecular weight hyaluronan, HA1500.

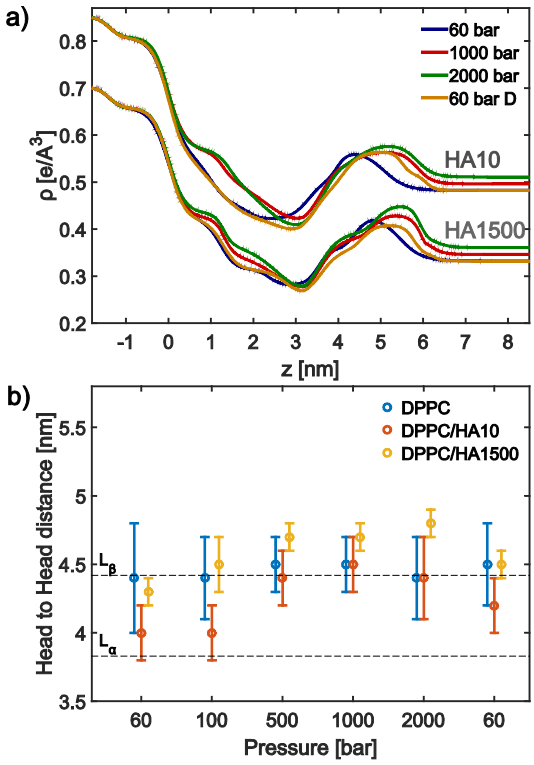

Figure 4 (a) Electron density profiles of DPPC/HA10 and DPPC/HA1500 composite samples at 39 °C and different pressures. Offset between data obtained in presence of HA10 and HA1500 for clarity. (b) Head-to-head distance of the samples measured at 39 °C as function of the hydrostatic pressure. The dashed lines show the head-to-head distance in the $L_{\beta'}$ phase (≈ 4.4 nm) and the L_α phase (≈ 3.8 nm).[1] The aqueous solution contained 150 mM NaCl and 10 mM $CaCl_2$.

DPPC+HA10

Compared to the profiles of the pure DPPC bilayer samples (see Figure 2a), the profiles of the sample composed of DPPC and HA10 at 39 °C (**Fehler! Verweisquelle konnte nicht gefunden werden.**a) exhibits a strong modification of the structure and a different response to high hydrostatic pressures. At 60 bar the bilayer shows less defined structures as also observed for the

lone DPPC bilayer at 55 °C. However, in presence of HA the electron density of the upper leaflet is increased giving rise to the already described asymmetry. An increase in pressure leads to a structural transition. At pressures of 500 bar and above the head-to-head distance is increased to 4.4 nm − 4.5 nm compared to 4.0 nm below 500 bar (as illustrated in **Fehler! Verweisquelle konnte nicht gefunden werden.**b), i.e. similar to pure DPPC bilayers in the L_α phase. For pressures ≥ 500 bar the structure of the lower leaflet becomes similar to that of the lone DPPC bilayer that is in the $L_{\beta'}$ phase at 39 °C, with a well-defined structure at the head group and the tail group region and a strong increase in electron density. The upper leaflet shows a larger width of the head group region and a higher electron density of the tail group region for all pressures (compared to the lower leaflet). Such an asymmetric vertical bilayer structure is not observed for pure DPPC bilayers, neither was such a structure observed for DPPC/HA composites in 150 mM NaCl solution in absence of $CaCl_2$.[34] As discussed above, the asymmetry is suggested to be due to HA chains accumulating between the DPPC molecules in the upper leaflet.

After the pressure was decreased to 60 bar (curve denoted 60 bar D) again, the structure also changed. The lower leaflet rearranged in to its original structure, while the structure of the upper leaflet kept the vertical structure it had at high pressures. Consequently, the head-to-head distance of the bilayer (4.2 nm) is in between that observed initially at 60 bar and later at 2000 bar. This suggests irreversible accretion of HA in the tail group region of the outer leaflet due to the reordering process. It is conceivable that the weakening of the hydrophobic interaction at high hydrostatic pressure[62] facilitates this incorporation of HA in the outer leaflet.

The structural transition for DPPC/HA10 composites at 39 °C, which occurs by increasing the pressure from 100 to 500 bar (Figure 4a), was unexpected as such a transition was not observed for pure DPPC.[34] Thus, for DPPC/HA10 at 39 °C and 60 bar the sample is in a different state

than the corresponding pure DPPC layer. We note that a discussion on the phase behaviour have to made with caution as the DPPC/HA system is a binary one and as HA penetrates the upper leaflet the phase diagram might be changed. However, it is clear that the bilayer structure and head-to-head distance of DPPC/HA10 at 39°C and 60 bar show more similarities to the DPPC sample at 55 °C which is in the L_α (see Figure 3b). It can be speculated that the resulting bilayer structure at 39 °C was, due to the suppressed ripple phase, in an energetically unfavourable state that, in combination with the disturbance of the lipid ordering by the HA, led to a modification of the phase state. The fact that both leaflets were disturbed might be explained by the low molecular weight of HA10 that is rod-like,[59] in contrast to the coiled structure of HA1500.[60, 61] Thus, HA10 could possibly also access the lower leaflet through small voids in the bilayer (as seen in the fluorescence microscopy images). After the transition the head-to-head distance increases to 4.4 − 4.5 nm, which corresponds to the $L_{\beta'}$ phase.[1] However, due to its asymmetry, the electron density profile and particularly that of the upper leaflet clearly deviates from the electron density profile of a typical bilayer.

DPPC and HA1500

The electron density profiles of the sample composed of DPPC and HA1500 at 39 °C are also shown in **Fehler! Verweisquelle konnte nicht gefunden werden.**a. Just as was observed in presence of HA10, the layer of DPPC and HA1500 is asymmetric with a higher electron density in the tail group region of the upper leaflet compared to that in the lower leaflet. Again the layer structure is more smeared than for the pure DPPC bilayer. Increasing the pressure from 60 to 1000 bar leads to an increase in the head-to-head distance by 0.4 nm (see **Fehler! Verweisquelle konnte nicht gefunden werden.**b) and an alteration of the vertical bilayer structure can be

observed. Especially for the lower leaflet an increase in the electron density can be seen which is accompanied by a more pronounced structure, which indicates a reduced overall roughness. A further increase of the hydrostatic pressure to 2000 bar caused mainly a higher electron density. Decreasing the pressure back to 60 bar restores the original structure of the lower leaflet, while the upper leaflet kept roughly the structure it had at high hydrostatic pressures (≥ 1000 bar).

The head-to-head distance of the sample composed of DPPC and HA1500 at 39 °C corresponds to the $L_{\beta'}$ phase at 60 bar, but at pressure at and above 500 bar (500 bar is the transition value between L_{α} and $L_{\beta'}$ for DPPC in bulk at 55 °C) it increases to 4.7 − 4.8 nm which is up to 0.4 nm larger than reported for the $L_{\beta'}$ phase.[1] Further, the shape of the electron density profile is not typical for a bilayer as it is highly asymmetric. These two findings hint at a structural decoupling of the two leaflets. Such a decoupling has also been suggested for mica supported DMPC and DPPC bilayers studied with AFM,[63-65] but it was not observed by XRR for DPPC bilayers on silica in contact with 150 mM NaCl solution.[34] Thus, it can be concluded that on silica it is facilitated by divalent Ca^{2+} ions that strengthens the DPPC-HA interaction. Further, it is known that $CaCl_2$ strengthens the binding between phospholipids and silica substrates [54]. The two leaflets are therefore in contact with two very different environments, that both strongly interact with the DPPC molecules.

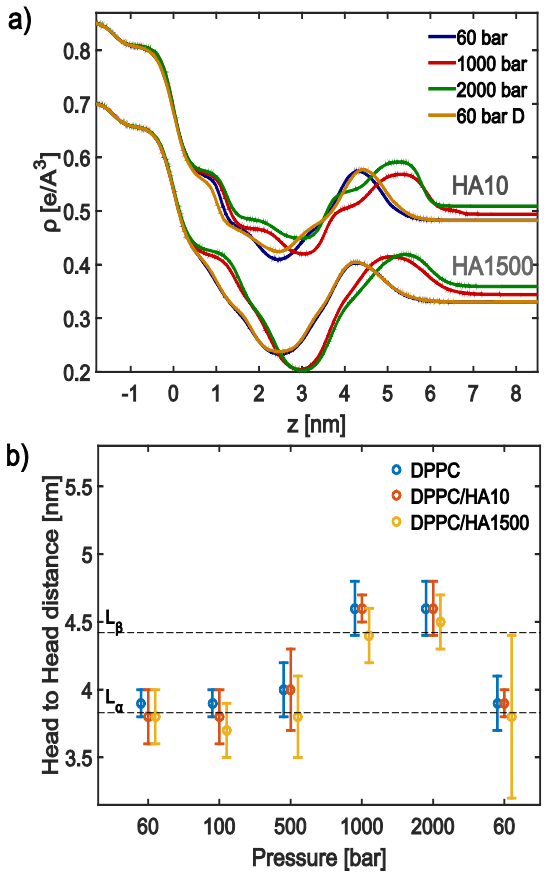

Figure 5 (a) Figure 5 (a) shows the electron density profiles of a sample composed of DPPC and HA10, which were measured at 55 °C. Like the profiles of pure DPPC bilayer (see Figure 2b) a clear bilayer structure could be seen, with a structural transition that occurs between 500 and 1000 bar (see supporting information S3). (b) The head-to-head distance of the DPPC/HA composite layers as function of the applied pressure. The aqueous solution contained 150 mM NaCl and 10 mM $CaCl_2$.

Structure of DPPC bilayer with adsorbed HA at high hydrostatic pressures at 55°C

In general the effect of HA on the DPPC bilayer structure is less pronounced at 55 °C compared to at 39 °C. At low pressures (≤ 500 bar) the bilayer structure for both DPPC+HA10 and DPPC+HA1500 is close to symmetric as shown in Figure 5a, and only the structure of the

lower leaflet is a little less distinct. In contrast, at high pressures (≥ 1000 bar) the upper leaflet shows a higher electron density compared to the lower leaflet. While the lower leaflet shows only an increase of the thickness (≈ 0.6 nm), the upper leaflet changes its structure considerably. A further increase in pressure to 2000 bar leads to an overall increase in electron density. After decreasing the pressure to 60 bar (curve denoted 60 bar D) again, the original structure of the bilayer is nearly restored. The head-to to-head distance of the bilayer increases with the hydrostatic pressure (from ≤ 500 bar to ≥ 1000 bar) from 4.0 nm to 4.5 nm, which can be seen in Figure 5b.

At 55 °C the head-to-head distances Figure 5b) do not hint at a difference in phase behaviour between DPPC/HA composites and DPPC bilayers. Below 500 bar the bilayers head-to-head distance corresponds well to a DPPC bilayer in the L_α phase.[1, 26, 32, 66] Furthermore, the DPPC/HA samples (Figure 5a) show less asymmetry as compared to at 39 °C. At pressures ≥ 1000 bar the bilayers show a head-to-head distance between 4.4 nm and 4.6 nm, corresponding to the $L_{\beta'}$ phase.[1] However, especially for DPPC/HA10 a strong asymmetry, as also observed for the samples at 39 °C, could be observed at pressures above the phase transition. Again, the two leaflets of the bilayer seem to be structurally decoupled.[63-65] The asymmetry only occurs at pressures and temperatures where the pure DPPC bilayer should be in the $L_{\beta'}$ phase. One reason could be defects in the bilayer that occurs as it transforms from the L_α to $L_{\beta'}$ phase where the area per lipid is smaller.[1, 54] Again HA10 shows the strongest effect. After releasing the pressure, the electron density profiles were restored to their original shape, i.e. the structural changes are completely reversible. This is in contrast to the measurements at 39 °C. A reason might be the

much higher flexibility and mobility of the lipids at 55 °C, which facilitates reorganization of the sample.[67]

Table 1 below summarizes our findings of the effects of HA of different molecular weights on the lateral structure of DPPC bilayers at different hydrostatic pressures. It compares the structure of the composite layer with that of the pure DPPC bilayer under similar temperature and pressure conditions.

Sample	T [°C]	P [bar]	Structure
DPPC	39	60-2000	Typical bilayer structure, $L_{\beta'}$
DPPC	55	60-500	Typical bilayer structure, L_{α}
DPPC	55	1000-2000	Typical bilayer structure, $L_{\beta'}$
DPPC+ HA10	39	60-2000	Distorted/smeared bilayer structure, smaller L_{α}–like head-to-head distance below 100 bar, higher electron density in upper than in lower leaflet. L_{α} to $L_{\beta'}$-like transition between 100 and 500 bar.
DPPC+ HA10	55	60-500	L_{α}-like phase. Slightly higher electron density in upper than in lower leaflet. Slightly better ordered bilayer compared to 39 °C
DPPC+ HA10	55	1000-2000	Higher electron density in upper than in lower leaflet
DPPC+ HA1500	39	60-2000	Distorted/smeared bilayer structure, higher electron density in upper than in lower leaflet. $L_{\beta'}$ - like structure, but larger head-to-head distance at pressures at and above 500 bar.
DPPC+ HA1500	55	60-500	L_{α}-like phase. Slightly higher electron density in upper than in lower leaflet.
DPPC+ HA1500	55	1000-2000	Higher electron density in upper than in lower leaflet. $L_{\beta'}$ - like phase

Table 1. Summary of the observations for DPPC and HA composite layers obtained from the XRR measurements under different conditions.

Conclusions

The fluorescent microscopy results of the present study show that HA adsorbs and form an inhomogeneous layer on silica DPPC bilayers, and this also results in a less homogeneous lateral distribution of DPPC over the surface. The higher molecular weight HA has a larger impact on the lateral distribution than the lower molecular weight HA. The effect observed here, in presence of 10 mM $CaCl_2$ and 150 mM NaCl, is larger than that reported in a previous study using 150 mM NaCl in absence of calcium ions.[34] Several techniques have previously been used to explore the effect of calcium ions on DPPC bilayers.[57, 68] and molecular information on alterations in structure and hydration has been obtained from VSFS measurements.[37, 57] Our XRR data demonstrate that $CaCl_2$ leads to an alteration of the vertical structure of the silica supported DPPC bilayer with and without adsorbed HA and hints at a modification of the phase diagram. Table 1 summarises our observations for the different conditions. Our findings reveal that low molecular weight HA has a stronger effect on the vertical structure of the bilayer than high molecular weight HA. An L_α –like phase can be observed for DPPC/HA layers in the presence of $CaCl_2$ at 39 °C which is below the phase transitionn of pure DPPC. At high pressure the presence of HA leads to a structural decoupling of the two leaflets of the DPPC bilayer and formation of asymmetric structures. Comparing these findings to the results of silica supported bilayers at high pressure in 150 mM NaCl solution show that addition of $CaCl_2$ leads to increase in the interaction of HA and DPPC, as the effect on the bilayer structure was much weaker in 150 mM NaCl solution. This is most likely caused by divalent Ca^{2+} ions, which induce favourable electrostatic interactions between HA and DPPC and possibly act as bridging agents between the DPPC head groups and the negatively charged carboxyl groups of HA.

Further, the addition of $CaCl_2$ clearly increased the robustness of DPPC bilayers against high hydrostatic pressures and also DPPC/HA composites, especially in the L_α phase (the biologically most relevant phase), retain their high resistance against structural defects at high pressures.

ASSOCIATED CONTENT

The supporting information contains the original data of the reflectivity curves along with the data fits.

AUTHOR INFORMATION

Corresponding Author

D.C.F. Wieland, Helmholtz Zentrum Geesthacht, Institute of Materials Research, Max-Planck-Straße, 21502 Geesthacht, Germany, email address: florian.wieland@hzg.de

Author Contributions

The manuscript was written by significant contributions of all authors. All authors have given approval to the final version of the manuscript. ‡These authors contributed equally. (match statement to author names with a symbol)

Funding Sources

Röntgen-Angström Cluster Joint

.

ACKNOWLEDGMENT

We acknowledge the BMBF Röntgen Angström Cluster JOINT (05K2012) for financial support. Further we thank Veijo Honkimaki, ESRF, Grenoble, for support during the beam time.

1. Nagle, J. F.; Tristram-Nagle, S., Structure of lipid bilayers. *Biochimica et Biophysica Acta (BBA) - Reviews on Biomembranes* **2000,** 1469, 1591195.
2. Hills, B. A., Surface-active phospholipid: a Pandora's box of clinical applications. Part II. Barrier and lubricating properties. *Internal medicine journal* **2002,** 32, (5-6), 242-51.
3. Schwarz, I. M.; Hills, B. A., Surface-active phospholipid as the lubricating component of lubricin. *Rheumatology* **1998,** 37, 21-26.
4. Hills, B. A., Surface-active phospholipid: a Pandora's box of clinical applications. Part II. Barrier and lubricating properties. *Internal Medicine Journal* **2002,** 32, (5-6), 242-251.
5. Murakami, T.; Yarimitsu, S.; Nakashima, K.; Yamaguchi, T.; Sawae, Y.; Sakai, N.; Suzuki, A., Superior lubricity in articular cartilage and artificial hydrogel cartilage. *Proceedings of the Institution of Mechanical Engineers, Part J: Journal of Engineering Tribology* **2014,** 228, (10), 1099-1111.
6. Klein, J., Hydration lubrication. *Friction* **2013,** 1, (1), 1-23.
7. Klein, J., Molecular mechanisms of synovial joint lubrication. *Proceedings of the Institution of Mechanical Engineers, Part J: Journal of Engineering Tribology* **2006,** 220, (8), 691-710.
8. Hills, B., Oligolamellar lubrication of joints by surface active phospholipid. *The Journal of Rheumatology* **1989,** 16, (1), 82-91.
9. Sivan, S.; Schroeder, A.; Verberne, G.; Merkher, Y.; Diminsky, D.; Priev, A.; Maroudas, A.; Halperin, G.; Nitzan, D.; Etsion, I.; others, Liposomes act as effective biolubricants for friction reduction in human synovial joints. *Langmuir* **2009,** 26, (2), 1107-1116.
10. Grant, L. M.; Tiberg, F., Normal and Lateral Forces between Lipid Covered Solids in Solution: Correlation with Layer Packing and Structure. *Biophysical Journal* **2002,** 82, 1373-1385.
11. Goldberg, R.; Schroeder, A.; Silbert, G.; Turjeman, K.; Barenholz, Y.; Klein, J., Boundary Lubricants with Exceptionally Low Friction Coefficients Based on 2D Close-Packed Phosphatidylcholine Liposomes. *Advanced Materials* **2011,** 23, 3517-3521.
12. Murakami, T.; Yarimitsu, S.; Nakashima, K.; Sawae, Y.; Sakai, N., Influence of synovia constituents on tribological behaviors of articular cartilage. *Friction* **2013,** 1, (2), 150-162.
13. Sarma, A. V.; Powell, G. L.; LaBerge, M., Phospholipid composition of articular cartilage boundary lubricant. *Journal of Orthopaedic Research* **2001,** 19, (4), 671-676.
14. Mahmoud, T., Hyaluronan and synovial joint:

function, distribution and healing. *Interdiscip Toxicol* **2013,** 6, 111-125.
15. Rutjes, A. W. S.; Jüni, P.; da Costa, B. R.; Trelle, S.; Nüesch, E.; Reichenbach, S., Viscosupplementation for Osteoarthritis of the Knee. *Annals of Internal Medicine* **2012,** 157, (3), 180.
16. Forsey, R. W. a. F., J. and Thompson, J. and Stone, M. H. and Bell, C. and Ingham, E., The effect of hyaluronic acid and phospholipid based lubricants on friction within a human cartilage damage model. *Biomaterials* **2006,** 27, 4581-4590.
17. Wang, M.; Liu, C.; Thormann, E.; Dedinaite, A., Hyaluronan and Phospholipid Association in Biolubrication. *Biomacromolecules* **2013,** 14, 4198-4206.

18. Liu, C.; Wang, M.; An, J.; Thormann, E.; Dėdinaitė, A., Hyaluronan and phospholipids in boundary lubrication. *Soft Matter* **2012,** 8, 10241-10244.
19. Raj, A.; Wang, M.; Zander, T.; Wieland, D. C. F.; Liu, X.; An, J.; Garamus, V. M.; Willumeit-Römer, R.; Fielden, M.; Claesson, P. M.; D?dinait?, A., Lubrication synergy: Mixture of hyaluronan and dipalmitoylphosphatidylcholine (DPPC) vesicles. *Journal of Colloid and Interface Science* **2017,** 488, 225-233.
20. Milas, M., Rinaudo Marguerite, Characterization and Properties of Hyaluronic Acid (Hyaluronan). In *Polysaccharides: Structural Diversity and Functional Versatility*, Dumitriu: 1998; pp 535-550.
21. Buhler, E.; Boue, F., Chain Persistence Length and Structure in Hyaluronan Solutions: Ionic Strength Dependence for a Model Semirigid Polyelectrolyte. *Macromolecules* **2004,** 37, (4), 1600-1610.
22. Scott, J. E.; Heatley, F., Hyaluronan forms specific stable tertiary structures in aqueous solution: A 13C NMR study. *Proceedings of the National Academy of Sciences* **1999,** 96, (9), 4850-4855.
23. Mero, A.; Campisi, M., Hyaluronic Acid Bioconjugates for the Delivery of Bioactive Molecules. *Polymers* **2014,** 6, (2), 346-369.
24. Nagle, J. F.; Tristram-Nagle, S., Structure of lipid bilayers. *Bba-Rev Biomembranes* **2000,** 1469, (3), 159-195.
25. Sun, W. J.; Suter, R. M.; Knewtson, M. A.; Worthington, C. R.; Tristramnagle, S.; Zhang, R.; Nagle, J. F., Order and Disorder in Fully Hydrated Unoriented Bilayers of Gel Phase Dipalmitoylphosphatidylcholine. *Phys Rev E* **1994,** 49, (5), 4665-4676.
26. Koynova, R.; Caffrey, M., Phases and phase transitions of the phosphatidylcholines. *Biochimica et Biophysica Acta (BBA)-Reviews on Biomembranes* **1998,** 1376, (1), 91-145.
27. Akabori, K.; Nagle, J. F., Structure of the DMPC lipid bilayer ripple phase. *Soft Matter* **2014,** 11, (5), 918-926.
28. Naumann, C.; Brumm, T.; Bayerl, T. M., Phase transition behavior of single phosphatidylcholine bilayers on a solid spherical support studied by DSC, NMR and FT-IR. *Biophysical journal* **1992,** 63, (5), 1314-1319.
29. Johnson, S.; Bayerl, T.; McDermott, D.; Adam, G.; Rennie, A.; Thomas, R.; Sackmann, E., Structure of an adsorbed dimyristoylphosphatidylcholine bilayer measured with specular reflection of neutrons. *Biophysical journal* **1991,** 59, (2), 289-294.
30. Alessandrini, A.; Facci, P., Phase transitions in supported lipid bilayers studied by AFM. *Soft Matter* **2014**, (37), 10, 7145-7146.
31. Harb, F.; Simon, A.; Tinland, B., Ripple formation in unilamellar-supported lipid bilayer revealed by FRAPP. *The European Physical Journal E* **2013,** 36, (12).
32. Winter, R.; Jeworrek, C., Effect of pressure on membranes. *Soft Matter* **2009,** 5, (17), 3157-3157.
33. Hodge, W.; Fijan, R.; Carlson, K.; Burgess, R.; Harris, W.; Mann, R., Contact pressures in the human hip joint measured in vivo. *Proceedings of the National Academy of Sciences* **1986,** 83, (9), 2879-2883.
34. Zander, T. Wieland., D.C. F. and Raj, A. and Wang, M. and Nowak, B. and Krywka, C. and Dedinaite, A. and Claesson, P. M. and Garamus, V. M. and Schreyer, A. and Willumeit-Römer, R.., The influence of hyaluronan on the structure of a DPPC - bilayer under high pressures. *Colloids Surfaces B Biointerfaces* **2016**, 142 230-238.
35. *Handbook of Biomaterial Properties*. Springer US: 1998.

36. Uhríková, D.; Kucerka, N.; Teixeira, J.; Gordeliy, V.; Balgavý, P., Structural changes in dipalmitoylphosphatidylcholine bilayer promoted by Ca 2+ ions: a small-angle neutron scattering study. *Chemistry and physics of lipids* **2008,** 155, 80-89.
37. Hua, W.; Verreault, D.; Allen, H. C., Solvation of Calcium-Phosphate Headgroup Complexes at the DPPC/Aqueous Interface. *Chemphyschem* **2015,** 16, (18), 3910-3915.
38. Wieland, F.; Degen, P.; Zander, T.; Gayer, S.; Raj, A.; An, J.; Dedinaite, A.; Claesson, P. M.; Willumeit-Römer, R., Structure of DPPC-hyaluronan interfacial layers - effects of molecular weight and ion composition. *Soft Matter* **2016** 12, (3), 729-740.
39. Dahl, L. B.; Dahl, I. M.; Engstrom-Laurent, A.; Granath, K., Concentration and molecular weight of sodium hyaluronate in synovial fluid from patients with rheumatoid arthritis and other arthropathies. *Annals of the Rheumatic Diseases* **1985,** 44, 817-822.
40. Kern, W.; Puotinen, D. A., Cleaning Solutions Based on Hydrogen Peroxide for use in Silicon Semiconductor Technology. *RCA Review* **1970,** 31, 187-206.
41. Kern, W., The Evolution of Silicon Wafer Cleaning Technology. *Journal of The Electrochemical Society* **1990,** 137, (6), 1887-1887.
42. Richter, R.; Mukhopadhyay, A.; Brisson, A., Pathways of Lipid Vesicle Deposition on Solid Surfaces: A Combined QCM-D and AFM Study. *Biophysical Journal* **2003,** 85, (5), 3035-3047.
43. Lind, T. K.; Cárdenas, M.; Wacklin, H. P., Formation of Supported Lipid Bilayers by Vesicle Fusion: Effect of Deposition temperature. *Langmuir* **2014,** 30, (25), 7259–7263.
44. Reichert, H.; Honkimäki, V.; Snigirev, A.; Engemann, S.; Dosch, H., A new X-ray transmission-reflection scheme for the study of deeply buried interfaces using high-energy microbeams. *Physica B: Condensed Matter* **2003,** 336, 46-55.
45. Wirkert, F. J.; Paulus, M.; Nase, J.; Möller, J.; Kujawski, S.; Sternemann, C.; Tolan, M., X-ray reflectivity measurements of liquid/solid interfaces under high hydrostatic pressure conditions. *J Synchrotron Radiat* **2014,** 21, (1), 76-81.
46. Gale, L. R.; Chen, Y.; Hills, B. A. C., Ross, Boundary lubrication of joints: Characterization of surface-active phospholipids found on retrieved implants. *Acta Orthopaedica* **2007,** 78, (3), 309-314.
47. Als-Nielsen, J.; Jacquemain, D.; Kjaer, K.; Leveiller, F.; Lahav, M.; Leiserowitz, L., Principles and applications of grazing incidence X-ray and neutron scattering from ordered molecular monolayers at the air-water interface. *Physics Reports* **1994,** 246, (5), 251-313.
48. Parratt, L., Surface Studies of Solids by Total Reflection of X-Rays. *Phys. Rev.* **1954,** 95, (2), 359-369.
49. Tolan, M., *X-Ray Scattering from Soft-Matter Thin Films*. Springer Berlin Heidelberg: 1999; Vol. 148.
50. Tanaka, M.; Girard, G.; Davis, R.; Peuto, A.; Bignell, N., Recommended table for the density of water between 0 °C and 40 °C based on recent experimental reports. *Metrologia* **2001,** 38, (4), 301-309.
51. Nagle, J. F.; Zhang, R.; Tristram-Nagle, S.; Sun, W.; Petrache, H. I.; Suter, R. M., X-ray structure determination of fully hydrated L alpha phase dipalmitoylphosphatidylcholine bilayers. *Biophysical Journal* **1996,** 70, 1419-1431.
52. Naumann, C.; Brumm, T.; Bayerl, T. M., Phase transition behavior of single phosphatidylcholine bilayers on a solid spherical support studied by DSC, NMR and FT-IR. *Biophysical journal* **1992,** 63, 1314-1319.

53. Johnson, S. J.; Bayerl, T. M.; McDermott, D. C.; Adam, G. W.; Rennie, A. R.; Thomas, R. K.; Sackmann, E., Structure of an adsorbed dimyristoylphosphatidylcholine bilayer measured with specular reflection of neutrons. *Biophysical journal* **1991,** 59, 289-294.
54. Tristram-Nagle, S.; Nagle, J. F., Lipid bilayers: thermodynamics, structure, fluctuations, and interactions. *Chemistry and Physics of Lipids* **2004,** 127, 3-14.
55. Aruga, S.; Kataoka, R.; Mitaku, S., Interaction between Ca2+ and dipalmitoylphosphatidylcholine membranes. *Biophysical Chemistry* **1985,** 21, 265-275.
56. Kataoka, R.; Aruga, S.; Mitaku, S.; Kinosita, K.; Ikegami, A., Interaction between Ca2+ and dipalmitoylphosphatidylcholine membranes. *Biophysical Chemistry* **1985,** 21, 277-284.
57. Casillas-Ituarte, N. N.; Chen, X. K.; Castada, H.; Allen, H. C., Na+ and Ca2+ Effect on the Hydration and Orientation of the Phosphate Group of DPPC at Air-Water and Air-Hydrated Silica Interfaces. *J Phys Chem B* **2010,** 114, (29), 9485-9495.
58. Richter, R. P.; Bérat, R.; Brisson, A. R., Formation of Solid-Supported Lipid Bilayers: An Integrated View. *Langmuir* **2006,** 22, 3497-3505.
59. Almond, A.; Brass, A.; Sheehan, J. K., Deducing polymeric structure from aqueous molecular dynamics simulations of oligosaccharides: predictions from simulations of hyaluronan tetrasaccharides compared with hydrodynamic and X-ray fibre diffraction data. *Journal of Molecular Biology* **1998,** 284, 1425-1437.
60. Mendichi, R.; Soltes, L.; Giacometti Schieroni, A., Evaluation of Radius of Gyration and Intrinsic Viscosity Molar Mass Dependence and Stiffness of Hyaluronan. *Biomacromolecules* **2003,** 4, 1805-1810.
61. Almond, A.; DeAngelis, P. L.; Blundell, C. D., Hyaluronan: The Local Solution Conformation Determined by NMR and Computer Modeling is Close to a Contracted Left-handed 4-Fold Helix. *Journal of Molecular Biology* **2006,** 358, 1256-1269.
62. Gross, M.; Jaenicke, R., Proteins under pressure. The influence of high hydrostatic pressure on structure, function and assembly of proteins and protein complexes. *European Journal of Biochemistry* **1994,** 221, 617-630.
63. Wu, H.-L.; Tong, Y.; Peng, Q.; Li, N.; Ye, S., Phase transition behaviors of the supported DPPC bilayer investigated by sum frequency generation (SFG) vibrational spectroscopy and atomic force microscopy (AFM). *Phys. Chem. Chem. Phys.* **2016,** 18, 1411-1421.
64. Charrier, A.; Thibaudau, F., Main Phase Transitions in Supported Lipid Single-Bilayer. *Biophysical Journal* **2005,** 89, 1094-1101.
65. Feng, Z. V.; Spurlin, T. A.; Gewirth, A. A., Direct Visualization of Asymmetric Behavior in Supported Lipid Bilayers at the Gel-Fluid Phase Transition. *Biophysical Journal* **2005,** 88, 2154-2164.
66. Braganza, L. F.; Worcester, D. L., Hydrostatic pressure induces hydrocarbon chain interdigitation in single-component phospholipid bilayers. *Biochemistry* **1986,** 25, 2591-2596.
67. Tamm, L. K.; McConnell, H. M., Supported phospholipid bilayers. *Biophysical Journal* **1985,** 47, 105-113.
68. Wieland, D. C. F.; Degen, P.; Zander, T.; Gayer, S.; Raj, A.; An, J. X.; Dedinaite, A.; Claesson, P.; Willumeit-Romer, R., Structure of DPPC-hyaluronan interfacial layers - effects of molecular weight and ion composition. *Soft Matter* **2016,** 12, (3), 729-740.